



Development of galangin-loaded nano-sized polyelectrolyte liposome: optimization and characterization

Büşra Karkar¹ · İlkyaz Patır¹ · Saliha Şahin¹

Received: 5 August 2022 / Revised: 26 November 2022 / Accepted: 5 May 2023 /
Published online: 24 May 2023

© The Author(s), under exclusive licence to Springer-Verlag GmbH Germany, part of Springer Nature 2023

Abstract

Galangin is a natural flavonol with high antioxidant properties and has a wide range characteristics of biological activity spectrum. Galangin has low solubility, permeability, and bioavailability, limiting its therapeutic use like many flavonoids. In this study, nano-sized polyelectrolyte liposomes were developed and characterized to overcome the properties that limit the use of galangin. The various parameters (phospholipid/solvent ratio, cholesterol/solvent ratio, time and galangin/solvent ratio) were optimized with a response surface methodology-central composite design to develop liposomes with maximum encapsulation efficiency using the thin-film hydration method. An optimum liposome formulation was developed with $93.77 \pm 0.05\%$ encapsulation efficiency, a spherical large unilamellar vesicle with a size of 485.5 ± 128.41 nm, and a zeta potential of -48 ± 7 mV. The optimum liposome formulation was coated with polyelectrolyte biopolymer chitosan (CH) and gum arabic (GUA) using the layer-by-layer deposition method to improve its stability and drug release profile. The CH-liposome has a size of 208.05 ± 73.04 nm and a zeta potential of $+40 \pm 5$ mV. The GUA-CH-liposome has a size of 266.60 ± 8.49 nm and a zeta potential of -6 mV. Fourier transform infrared spectroscopy analysis showed that galangin was encapsulated without disturbing the liposome structure and the polyelectrolyte coated the surface with electrostatic interaction. At the end of the in vitro release study, GUA-CH-liposome released 23.84% of galangin. Regarding stability, drug loading capacity of GUA-CH-liposome, which was $93.77 \pm 0.05\%$ on day 0, changed to $92.72 \pm 0.51\%$ at $+4$ °C, $93.09 \pm 0.01\%$ at room temperature and $93.15 \pm 0.01\%$ at -24 °C on day 28.

Keywords Liposome · Polyelectrolyte · Optimization · Galangin · Encapsulation

Introduction

Galangin (3,5,7-trihydroxyflavone, GA) is a natural bioactive flavonol, which belongs to the class of flavonoids, and is the main component of *Alpinia officinarum* Hance (AO) [1]. The flavonoid ring of galangin indicates high antioxidant activity [2], and this has been studied and published many times before. In addition to this antioxidant activity, galangin shows a wide range of characteristics of biological activity spectrum such as antimicrobial, anti-viral, anti-inflammatory, anti-mutagenic, and anti-tumor activities [3]. In contrast to all its biological activities, galangin has limited therapeutic use due to its low solubility in water, oxidative instability, low permeability, as well as low bioavailability [4].

Encapsulation is a technique that focuses on increasing bioavailability, solubility, stability, protection from environmental factors, and controlled drug release [5] of bioactive compounds such as polyphenols, which are suitable for use in many fields but have low bioavailability. This technique involves producing nano- or micro-dimension capsules [6] by covering bioactive compounds with a wall material, e.g., carbohydrate, lipid, or polymer. The encapsulation process is divided into two categories: microencapsulation, in which capsules are formed in the range of 1–1000 μm , and nanoencapsulation, in which capsules are formed in the range of 1–1000 nm [7]. Nanoencapsulation has been used in many fields for many years as it significantly advances encapsulation efficiency, drug loading capacity, targeting, stability, bioavailability, and a controlled release profile [8]. Using this technique, nano-sized drug delivery systems can be developed and generated such as particles, capsules, niosomes, spheres, emulsions, micelles, and liposomes [9].

Liposomes are spherical lipid vesicles composed of an aqueous core and one or more lipid bilayer shells [10]. They consist of two basic components; phospholipids and cholesterol [11]. Phospholipids are amphiphilic molecules consisting of a polar head and a nonpolar tail [12]. During liposome formation, the phospholipid molecules form a bilayer and surround the aqueous phase, while the cholesterol molecules are embedded in the bilayer structure [13]. Eventually, a spherical liposome with an aqueous core and a phospholipid bilayer shell is formed, and cholesterol molecules stabilize the liposome structure [14]. This liposome structure is like an imitation of a biological cell membrane and can encapsulate both hydrophilic and hydrophobic bioactive compounds; hydrophilic compounds are embedded in the core and hydrophobic compounds are embedded in the wall material [15]. Thus, it easily transports bioactive compounds with different structures and solubility to biological cells [16].

Liposomes are biodegradable, biocompatible, non-toxic, targeted, and easily functionalized [17]. Liposomes, despite all “their” good properties, had low stability and are easily affected by environmental conditions due to fast hydrolysis and oxidation of lipids [18]. The coating of liposomes provides a solution to their low stability problem and preserves the physical and chemical properties of liposomes and can change charge, size, and morphology [19]. For this purpose, biopolymers such as chitosan, alginate, gum arabic [20] and synthetic polymers such as polyethylene glycol (PEG) and polyvinyl alcohol are often used as coating materials [21]. The

most commonly used method for coating liposomes is LbL deposition. This method is based on the electrostatic deposition of oppositely charged coating materials and liposomes can be coated with one or more layers using this method [22].

In the last decade, galangin-loaded niosomes [23], polymeric micelles [24], nanostructured lipid carriers [25], liposomes [26], nanoparticle [27], and PEG-modified liposomes [28] have been developed. However, no galangin-loaded polyelectrolyte biopolymer (chitosan-gum arabic)-coated liposomes have been developed. The aim of this study is to obtain maximum encapsulation efficiency by optimizing various parameters (phospholipid/solvent ratio, cholesterol/solvent ratio, time and galangin/solvent ratio) for the production of galangin-loaded liposomes by using response surface methodology. Optimum liposome formulation (O-liposome) was coated with polyelectrolyte biopolymer by LbL deposition and their sizes, zeta potentials, polydispersity index, surface morphologies, stability, and in vitro drug release were characterized.

Material and method

Materials

Ethanol, formic acid, and acetic acid were purchased from Merck (Darmstadt, Germany). Acetonitrile in HPLC grade, Chitosan (Medium molecular weight), Gum arabic from the acacia tree, and Cholesterol were purchased from Sigma-Aldrich (St. Louis, MO., USA). Lecithin (L- α -phosphatidylcholine) from soybean was purchased from Tito (İzmir, Turkey). AO root powder was purchased from a local market in Bursa, Turkey.

Method

Extraction of galangin

The extraction of galangin from *Alpinia officinarum* was prepared as described by Li et al., 2022 with little modifications. 20 g of AO root powder and 100 mL of absolute ethanol were placed in a glass flask at room temperature for 4 h in a magnetic stirrer. The ethanolic extract was then filtered through a filter paper and separated from the solid phase and it was stored at 4 °C until use [29].

High performance liquid chromatography (HPLC–DAD)

The Agilent 1200 Series HPLC–DAD system including an autosampler, vacuum degasser, and binary pump and diode array detector was used for the chromatographic analysis of GA in AO root powder. The chromatographic separations were performed using an XBridge C18 (4.6×250 mm, 3.5 μ m) column from Waters (USA). The mobile phase contains 1% formic acid (solvent A) and acetonitrile (solvent B) in water and the gradient conditions are as follows: 0–10 min 13%

B, 10–20 min 41.5% B, 20–25 min 70% B, 25–35 min 10% B. The flow rate was 0,6 ml/min, the injection volume was 20 μ L and the total run time for the analysis was 35 min [30].

Encapsulation efficiency

Encapsulation efficiency is determined by the chromatographic method. Liposome formulations were centrifuged at 4500 g for 2 h. After centrifugation, the amounts of GA remaining in the supernatant were determined by the HPLC. Encapsulation efficiency was determined by this equation:

Encapsulation efficiency (%) = $(\text{The initial amount of GA} - \text{The remaining amount of GA} / \text{The initial amount of GA}) \times 100$.

Preparation of liposome

The liposome formulation was prepared as described by Zhu (2018) with little modifications by the thin-film hydration method. Briefly, lecithin (phospholipid, PC) solution (1–9 mg:mL), cholesterol (CHOL) solution (0.2–1.8 mg:mL), and GA solution (0.1–0.5 mg:mL) were dissolved in absolute ethanol in a boiling flask with a final volume of 25 mL and the solution was kept in an ultrasonic bath at 40 °C in the range of 15–55 min. After the ultrasonic bath, the solvent was evaporated at 55 °C using a rotary evaporator and a clear lipid film was obtained. The lipid film was hydrated with 10 mL of ultrapure water and filtered through a 0.45 μ m poly(vinylidene fluoride) filter and stored at 4 °C [26].

Experimental design

RSM is an experimental statistical technique that uses quantitative data from experiments to explain multivariate scenarios simultaneously with multiple regression analysis [31]. In this study, four parameters such as PC/solvent ratio, CHOL/solvent ratio, time, and GA/solvent ratio were examined. The responses of combinations of parameters were studied using a CCD to determine optimum conditions for maximum encapsulation efficiency. The range of independent parameters studied for CCD design is given in Table 1.

The total number of experiments (N) in a CCD can be calculated using Eq. (1):

$$N = 2^k + 2k + x_0 \quad (1)$$

where k represents the number of variables, x_0 is the replication number of the center point. In this study, a five-level, four-factor CCD was applied, which required thirty experiments for the optimization of liposome production parameters. Thirty experiments were performed to optimize the liposome production parameters according to Table 1. Twenty-four of these experiments were designed with six replications to assess pure error. After applying multiple regression analysis to the experimental data, Eq. (2) containing all interaction terms was used to calculate the predicted response:

Table 1 CCD of factors with coded values (PC, phosphatidylcholine; CHOL, cholesterol; GA, galangin)

Treatment	Factors			
	x_1	x_2	x_3	x_4
	PC/solvent ratio (mg:mL)	CHOL/solvent ratio (mg:mL)	Time(min)	GA/solvent ratio (mg:mL)
1	3	0.6	25	0.11
2	7	0.6	25	0.11
3	3	1.4	25	0.11
4	7	1.4	25	0.11
5	3	0.6	45	0.11
6	7	0.6	45	0.11
7	3	1.4	45	0.11
8	7	1.4	45	0.11
9	3	0.6	25	0.22
10	7	0.6	25	0.22
11	3	1.4	25	0.22
12	7	1.4	25	0.22
13	3	0.6	45	0.22
14	7	0.6	45	0.22
15	3	1.4	45	0.22
16	7	1.4	45	0.22
17	1	1	35	0.165
18	9	1	35	0.165
19	5	0.2	35	0.165
20	5	1.8	35	0.165
21	5	1	15	0.165
22	5	1	55	0.165
23	5	1	35	0.055
24	5	1	35	0.275
25	5	1	35	0.165
26	5	1	35	0.165
27	5	1	35	0.165
28	5	1	35	0.165
29	5	1	35	0.165
30	5	1	35	0.165

$$y = b_0 + \sum_{i=1}^4 b_i x_i + \sum_{i=1}^4 b_{ii} x_i^2 + \sum_{i=1}^3 \sum_{j=i+1}^4 b_{ij} x_i x_j \tag{2}$$

where y is the response, b_0 is the constant, b_i , b_{ii} , b_{ij} are linear, quadratic, and interaction effects, respectively, and x_i and x_j are independent variables.

The Design Expert 7.0.0 software (Stat-Ease Inc., USA) was used for statistical analysis results, and analysis variance (ANOVA), regression analysis, and drawing

of response surface plots were performed to determine optimal conditions for liposome production.

Coating of optimum liposome with polyelectrolyte

The coating of O-liposomes with CH (polycation) and GUA (polyanion) was prepared as described by Ciu (2021) with modifications and LbL deposition in two steps. Briefly, fresh CH solutions were prepared by dissolving CH in 1% glacial acetic acid aqueous solution at a concentration of 0.625%, and fresh GUA solutions were prepared in ultrapure water at a concentration of 2%. Both of the solutions were stirred overnight and adjusted to pH 5.5 followed by filtration. The first layer was accumulated by the addition of the O-liposome into the CH solution (1:1, v/v) dropwise with a syringe and mixing slowly for 1 h. The second layer was accumulated by the same procedure; the derived CH-liposomes were added dropwise with a syringe to the GUA solution (1:1, v/v) and mixed slowly for 1 h and the derived GUA-CH-liposomes pH was adjusted to 5.5 and centrifuged at 3000 g for 30 min [32].

Characterization of liposome

The characterization of liposome formulations was studied by an FTIR spectrometer (PerkinElmer, Spectrum 100, USA). The surface morphology of liposome formulations was studied by FE-SEM (Field-Emission Scanning Electron Microscopy, Carl Zeiss Gemini, Germany) at 3 kV (In BTU-MERLAB). Lyophilized liposome formulations were placed on aluminum plates and covered with gold. The average size and zeta potential of liposomes were measured at 25 °C using a dynamic light scattering (DLS) instrument Malvern Zetasizer Nano-ZS (Malvern Instruments, UK).

In vitro drug release

GA releases of liposome formulations were investigated using the dialysis method. In brief, liposome formulations and AO extract containing 4.75 mg/mL galangin (liposomes contain 4.75 mg/mL galangin) as control were filled into dialysis bags (14,000 MWCO, BioBasic, Canada) and immersed in phosphate-buffered saline medium at 37 °C, pH 7.4. The medium was stirred at 100 rpm until the end of 300 min and kept at 37 °C. Aliquots of the medium were collected from the immersion medium at intervals of 0 – 300 min and GA released from the liposome formulations was measured at 360 nm by the UV-Vis spectrophotometer. The concentration of GA released from the liposomes was found by the standard GA calibration curve [33].

Stability study

The stability of the liposome formulations was determined based on their drug loading capacity (%) (GA loading capacity of liposomes) at three different temperatures, in the range of 1–28 days. Briefly, liposome formulations were stored at +4 °C, −24 °C, and room temperature for 28 days. The samples were collected at different time intervals for 28 days and the drug loading capacity was determined at 360 nm in a UV-Vis spectrophotometer [20].

Drug loading capacity (%) = $(\text{The initial concentration of GA} - \text{The remaining concentration of GA}) / \text{The initial concentration of GA} \times 100$.

Result and discussion

Fitting the models

The liposome production parameters were optimized using CCD associated with RSM. The most favorable combination of variables includes PC/solvent ratio (1–9 mg:mL), CHOL/solvent ratio (0.2–1.8 mg:mL), time (15–55 min), and GA/solvent ratio (0.1–0.5 mg:mL) which were investigated for liposome production. The coded values, experimental and predicted percentage of encapsulation efficiency (explained in “[Encapsulation efficiency](#)” section) are given in Table 2.

Among the 30 experiments, 6 of which replicates, experiment 17 (PC/solvent ratio; 1 mg:mL, CHOL/solvent ratio; 1 mg:mL, time; 35 min, GA/solvent ratio; 0.3 mg:mL) showed the highest encapsulation efficiency of 93.19% and experiment 23 (PC/solvent ratio; 5 mg:mL, CHOL/solvent ratio; 1 mg:mL, time; 35 min, GA/solvent ratio; 0.1 mg:mL) showed the lowest encapsulation efficiency of 7.87%.

The Design Expert program (version 7.0.0) was used to calculate the effects and interactions of each variable. Fitting the experimental data with several models and analysis of variance (ANOVA) demonstrated that the encapsulation efficiency is best identified by a quadratic polynomial model. According to Table 3, the quadratic polynomial model, with a *p* value of less than 0.0001 from ANOVA, is qualified to illustrate the actual relationship between the response and the significant parameters. The model *F* value of 75.63 demonstrates that the model is in the 95% confidence interval.

Response surface analysis

The effects of factors such as PC/solvent ratio, CHOL/solvent ratio, time, and GA/solvent ratio for the production of liposomes were investigated. The response surface analysis shows that the relationship between encapsulation efficiency and liposome production parameters (Table 3) such as PC/solvent ratio, CHOL/solvent

Table 2 CCD of factors with experimental and predicted values

Treatment	Encapsulation efficiency (%)	
	Experimental	Predicted
1	34.43	34.04
2	21.38	23.64
3	40.52	40.63
4	20.83	17.22
5	30.14	29.91
6	21.30	21.83
7	32.88	35.38
8	12.34	14.31
9	53.87	53.43
10	32.08	28.51
11	71.02	69.42
12	29.75	31.50
13	41.48	44.02
14	20.02	21.44
15	59.64	58.91
16	24.00	23.32
17	93.19	92.55
18	46.37	46.56
19	19.43	18.60
20	26.70	27.07
21	26.93	29.91
22	21.02	17.59
23	7.87	6.54
24	34.06	34.94
25	19.29	18.96
26	14.64	18.96
27	16.56	18.96
28	22.24	18.96
29	17.73	18.96
30	23.32	18.96

Table 3 Analysis of variance (ANOVA) for the fitted quadratic polynomial model for optimization of liposome production parameters

Source	Liposome production ($R^2 = 0.9860$)				
	DF	SS	MS	F value	p value
Model	14	9676.57	691.18	75.63	< 0.0001
Lack of fit	10	81.20	8.12	0.73	0.6887
Pure error	5	55.89	11.18		

DF Degree of freedom; SS Sum of squares; MS Mean square

Table 4 Second-order polynomial equations and regression coefficients of the response variables

Responses	Second-order polynomial equations
Encapsulation efficiency (%)	$y = 44.26 - 22.38x_1 + 9.17x_2 - 7.03x_3 + 19.53x_4 - 3.25x_1x_2 - 7.26x_1x_4 - 4.70x_2x_4 + 12.65x_1^2$

x_1 PC/solvent ratio; x_2 CHOL/solvent ratio; x_3 Time; x_4 GA/solvent ratio

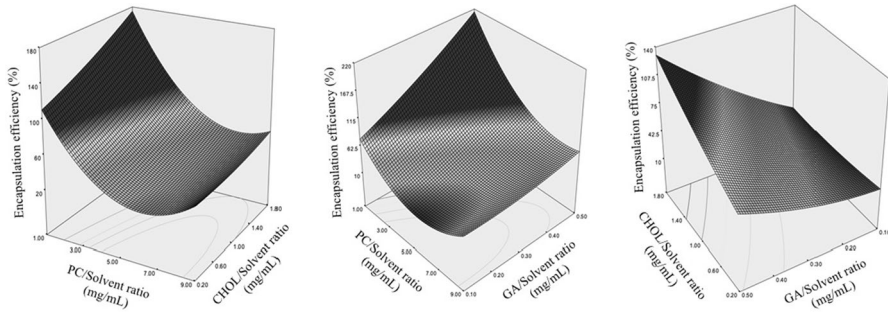


Fig. 1 Response surface plots of liposome production showing the effects of **a** PC/solvent ratio and CHOL/solvent ratio, **b** PC/solvent ratio and GA/solvent ratio, and **c** CHOL/solvent ratio and GA/solvent ratio on the encapsulation efficiency

ratio, time, and GA/solvent ratio is quadratic and has a good regression coefficient ($R^2 = 0.9860$).

In terms of encapsulation efficiency, the significant factors (p value < 0.05) in liposome production are $x_1, x_2, x_3, x_4, x_1x_2, x_1x_4, x_2x_4, x_1^2$, and the least effective factors are $x_1x_3, x_2x_3, x_3x_4, x_2^2, x_3^2, x_4^2$. The PC/solvent ratio, x_1 (p value < 0.0001), and its quadratic term of the PC/solvent ratio, x_1^2 (p value < 0.0001) are the most important factors affecting encapsulation efficiency (Table 4). PCs are the main components of liposomes, so the PC/solvent ratio is much more important than CHOL/solvent, GA/solvent, and time.

The significant interactions between liposome production parameters and encapsulation efficiency are illustrated by response surface plots. Figure 1a demonstrates the effects of the PC/solvent ratio and CHOL/solvent ratio, Fig. 1b PC/solvent ratio and GA/solvent ratio, Fig. 1c CHOL/solvent ratio and GA/solvent ratio on encapsulation efficiency, and their reciprocal effects.

In Fig. 1a, both CHOL/solvent ratio and PC/solvent ratio are effective in increasing encapsulation efficiency, if the CHOL/solvent ratio is kept constant and the PC/solvent ratio decreases, the encapsulation efficiency decreases, but if the PC/solvent ratio is reduced further, then the encapsulation efficiency begins to increase. The highest encapsulation efficiency is observed in the lowest PC/solvent ratio and CHOL/solvent ratio. The PC/solvent ratio has a negative effect on increasing encapsulation efficiency, while the CHOL/solvent ratio has a positive effect [34]. It is undesirable for the amount of PC to be too high for liposome formation because as the amount of PC increases, the amount of CHOL also increases to stabilize the

liposome being formed. CHOL molecules increase encapsulation efficiency by providing better packaging of lipid molecules for liposome formation [21].

In Fig. 1b, the encapsulation efficiency decreases when the GA/solvent ratio is kept constant and the PC/solvent ratio decreases, but the encapsulation efficiency begins to increase when the PC/solvent ratio reduces. The highest encapsulation efficiency is observed in the lowest PC/solvent ratio and highest GA/solvent ratio, and the lowest encapsulation efficiency is observed in the lowest GA/solvent ratio and highest PC/solvent ratio. The PC/solvent ratio negatively affects encapsulation efficiency and a high PC ratio is not desired for increasing encapsulation efficiency [34]. In addition, an increase in the PC ratio contributes to the generation of larger-size liposomes, which is undesirable in liposome formation [35].

In Fig. 1c, the ratio of CHOL/solvent ratio and GA/solvent ratio equally affect encapsulation efficiency and these have contrary effects. If the CHOL/solvent ratio is kept constant and the GA/solvent ratio is increased, the encapsulation efficiency decreases, but if the GA/solvent ratio is kept constant and the CHOL/solvent ratio is increased, the encapsulation efficiency increases. The highest encapsulation efficiency is observed in the highest CHOL/solvent ratio and the highest GA/solvent ratio. An increase in the amount of CHOL in the composition of the liposome causes the structure to become more rigid [36]. With high rigidity, the permeability of the lipid bilayer is reduced and drug leakage is prevented, resulting in high encapsulation efficiency. CHOL molecules increase hydrophobicity in the middle region of the lipid bilayer of liposomes, causing spaces between the lipid chains. This simplifies the entrapment of hydrophobic molecules in the spaces in the lipid bilayer and increases the encapsulation efficiency [37]. GA is a hydrophobic molecule and the encapsulation efficiency of GA increased with the increase in the CHOL/solvent ratio.

Optimization of liposome production variables

Table 5 demonstrates the optimum conditions, predictions, and experimental response for liposome production. The optimal condition for the production of liposomes is as follows: The PC/solvent ratio is 1.50 mg:mL, the CHOL/solvent ratio is 0.88 mg:mL, the time is 24.73 min, and the GA/solvent ratio is 0.19 mg:mL and the estimated percent of encapsulation efficiency at optimum conditions is 93.77%. In this study, the percentage of encapsulation efficiency obtained under optimum conditions was $93.77 \pm 0.05\%$. This result indicates that the experimental response and the predicted response are a fit. This fit verifies the validity of the model at the 95% confidence interval. Hence, the CCD model is accurate and reliable in predicting the maximum encapsulation efficiency for the production of liposomes.

Table 5 Optimum conditions, predicted and experimental values of responses

Responses	Maximum values		Optimum liposome production conditions			
	Predicted	Experimental	PC/solvent ratio (mg:mL)	CHOL/solvent ratio (mg:mL)	Time (min)	GA/solvent ratio (mg:mL)
Encapsulation efficiency (%)	93.77	93.77 ± 0.05	1.50	0.88	24.73	0.19

PC Phosphatidylcholine; *CHOL* Cholesterol; *GA* Galangin

Table 6 The actual size, hydrodynamic size, zeta potential, and polydispersity index of liposome formulations

Sample	Actual size (nm)*	Hydrodynamic size (nm)**	Zeta potential (mV)**	PDI**
O-Liposome	485.5 ± 128.41	234.4 ± 113.4	-48 ± 7	0.373 ± 0.035
CH-Liposome	208.05 ± 73.04	245.7 ± 249.3	+40 ± 5	0.389 ± 0.115
GUA-CH-Liposome	266.60 ± 8.49	567 ± 113	-6 ± 4	0.749 ± 0.272

O Optimum; CH Chitosan; GUA Gum arabic; PDI Polydispersity index

*Measured by FE-SEM

**Measured by DLS

Characterization of liposome formulations

The size of liposomes plays an important role in many aspects such as their intended use, targets, and the environmental behavior of liposomes. Thin-film hydration method was used in the preparation of liposomes, and one of the major disadvantages of this method is the formation of large-sized liposomes [38]. The hydrodynamic size of the O-liposome is 234.4 ± 113.4 nm, CH-liposome is 245.7 ± 249.3 nm, and GUA-CH-liposome is 567 ± 113 nm (Table 6). The O-liposome is a large unilamellar vesicle (LUV) with one lipid bilayer. The coating of the O-liposome with chitosan as the first layer resulted in a small increase in average size, but coating with gum arabic as the second layer resulted in a major increase in average size. The reason for this increase in size with the coating is the swelling of chitosan and gum arabic and the formation of agglomeration. In addition, hydrodynamic diameter is used as the average size, an agglomeration of liposomes in aqueous media, polymers adsorbed to the liposome surface and swelling may result in deviations from the actual liposome size.

The zeta potential value is an important factor in the stability of liposomes and their adsorption from the cell membrane [39]. If the zeta potential is more negative than -30 mV, the liposome is anionic, if it's more positive than $+30$ mV, the liposome is cationic, and if it's between -10 mV and $+10$ mV, the liposome is neutral [40]. The zeta potential of the O-liposome is -48 ± 7 mV and its anionic liposome. The negative zeta potential is as expected due to the use of negatively charged lecithin as the wall material of the liposome. The zeta potential of the CH-liposome is $+40 \pm 5$ mV and it's a cationic liposome. By coating the negatively charged liposome with CH, the zeta potential value changed from -48 ± 7 mV to $+40 \pm 5$ mV. This zeta potential is due to the positively charged nature of CH. The zeta potential of the GUA-CH-liposome is -6 ± 4 mV and it's a neutral liposome. The zeta potential value changed from $+40 \pm 5$ mV to -6 ± 4 mV by coating the positively charged CH-liposome with negatively charged GUA (Table 6). Similarly, Cui et al. [32], reported that the zeta potential increased from -16.44 mV to $+22.04$ mV when coating Chito-oligosaccharide-loaded liposomes with a polycation, chitosan, and decreased to -29.75 mV when coated with polyanion sodium alginate. However, sodium alginate has a

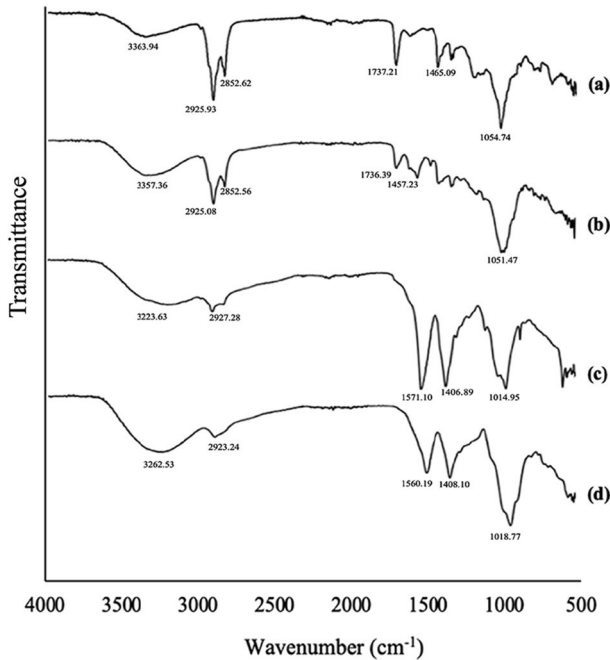


Fig. 2 FTIR spectrum of **a** empty liposome, **b** O-liposome, **c** CH-liposome, and **d** GUA-CH-liposome

higher ζ_{max} than GUA due to its structural differences [41]. Therefore, Cui et al.’s liposomes have negative zeta potential after coating with sodium alginate, whereas our liposomes have neutral zeta potential after GUA coating. Liposomes with negative and positive zeta potentials are pH-dependent and have restricted use in various environments, but neutral liposomes show full charge alteration depending on environmental pH [42]. This feature increases the use of neutral liposomes in a variety of environments.

The polydispersity index describes the size distribution of particles [43]. A polydispersity index between 0 and 0.5 indicates that the vesicles are monodisperse and homogeneous, while a value between 0.5 and 1 indicates that the vesicles are polydisperse and heterogeneous [44]. The polydispersity index of the O-liposome is 0.373 ± 0.035 and that of the CH-liposome is 0.389 ± 0.115 ; the O-liposome and CH-liposome are monodisperse and show one-dimensional distribution. The polydispersity index of GUA-CH-liposome is 0.749 ± 0.272 , GUA-CH-liposome is polydisperse and has a different dimensional distribution.

The chemical structures of the liposome formulations were characterized by FTIR. Figure 2 shows the FTIR spectrum of the liposome formulations. The empty liposome (Fig. 2a) shows O–H stretching band at 3363.94 cm^{-1} , the characteristic CH_2 stretching band at 2925.93 and 2852.62 cm^{-1} , C=O stretching band at 1737.21 cm^{-1} , C–H bending at 1465.09 cm^{-1} and 1054.74 cm^{-1} at P–O–C stretching band. The O-liposome (Fig. 2b) shows a broad O–H stretch band at 3357.36 cm^{-1} [45]. The hydrogen bonds formed by loading GA into empty liposomes increased

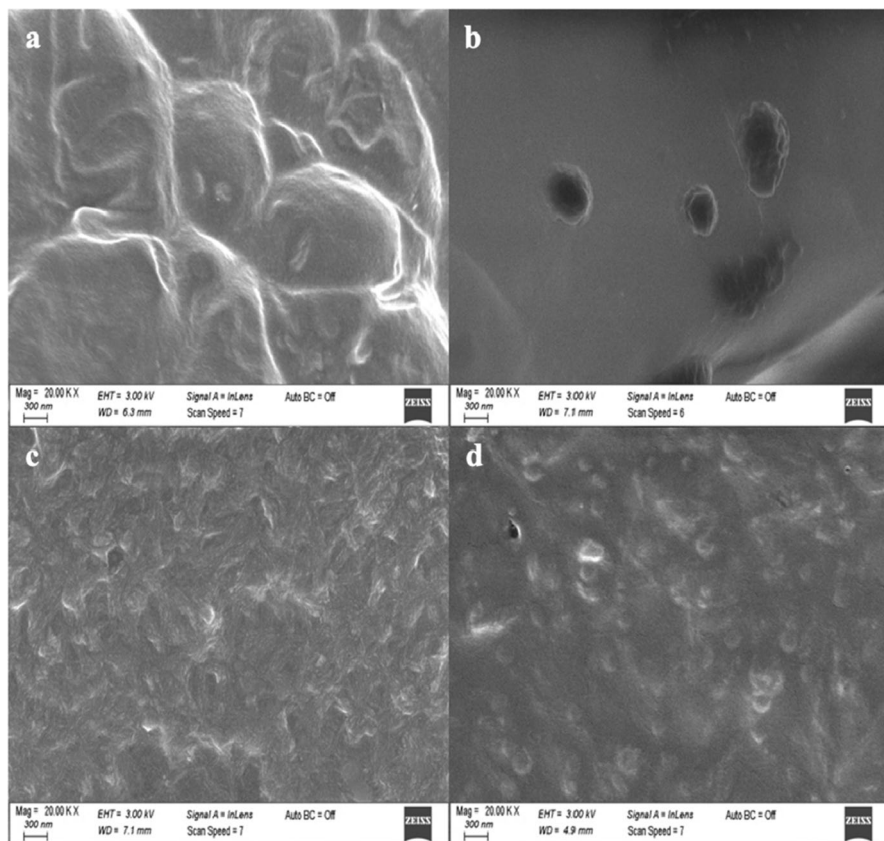


Fig. 3 FE-SEM image of **a** empty liposome **b** O-liposome **c** CH-liposome and **d** GUA-CH-liposome

the intensity while shifting the low-intensity O–H band at 3363.94 cm^{-1} in the empty liposome to 3357.36 cm^{-1} . In addition to the O–H stretching band, the CH_2 stretching bands in the O-liposome shifted to 2925.08 cm^{-1} and 2852.56 cm^{-1} , C=O stretching band 1736.39 cm^{-1} , C–H bending 1457.23 cm^{-1} and their intensity decreased. The P–O–C stretching band, which was at 1054.74 cm^{-1} in the empty liposome, shifted to 1051.47 cm^{-1} in the O-liposome and its intensity increased. The loading of GA into the empty liposome caused minor changes without disrupting the structure. The CH-liposome (Fig. 2c) shows a broad O–H stretching band masking the N–H stretching band at 3223.63 cm^{-1} , characteristic C–H stretching band of chitosan at 2927.28 cm^{-1} , C–O and C–N stretching bands at 1571.10 cm^{-1} , O–H and C–H vibrations at 1406.89 cm^{-1} and C–O stretch band at 1014.95 cm^{-1} [46]. The GUA-CH-liposome (Fig. 2d) shows a strong O–H stretching band masking the N–H stretching band at 3262.53 cm^{-1} the C–H stretching band at 2923.24 cm^{-1} , and the C–O stretching band at 1014.95 cm^{-1} , which is the characteristic band of GUA. The characteristic high-intensity C–N stretching bands of chitosan at 1571.10 cm^{-1} and 1406.89 cm^{-1} shifted to 1560.19 cm^{-1} and

1408.10 cm^{-1} , and their intensity greatly decreased. This is due to the electrostatic interaction between the $-\text{COO}^-$ group of gum arabic and the $-\text{NH}_2$ group of chitosan [47]. Rajabi et al. [48] observed similar shifts and changes in band intensities in the FTIR spectrum of chitosan-gum arabic nanocarriers and reported that this may be due to the electrostatic interaction between the negative and positive groups of GUA and CH.

The morphology of the liposome formulations was assessed by the FE-SEM technique. Figure 3 shows FE-SEM images of liposome formulations. The surface property, homogeneity, distribution, and size of liposomes are defined by their morphology. Morphology is directly related to the development and modification of the various properties of liposomes as drug carriers and application areas, and target sites [49]. In Fig. 3a, the empty liposome has a nearly spherical shape and its actual size was determined as 288.90 ± 78.91 nm (Table 6). The empty liposome is agglomerated and the liposomes appear to be embedded in the surface and do not have a regular structure. In Fig. 3b, the O-liposome has a spherical, regular structure and its actual size is determined as 485.5 ± 128.41 nm. However, the loading of GA into the empty liposome caused an increase in size. In Fig. 3c, the CH-liposome has a slightly spherical shape, the structure is not regular because it is agglomerated and does not have a homogeneous distribution, and its actual size is determined as 208.05 ± 73.04 nm. Coating of the O-liposome with CH resulted in a reduction in size, although the structure was irregular. In Fig. 3d, the GUA-CH-liposome has a generally regular structure and spherical shape, and its actual size was determined as 266.60 ± 8.49 nm. Coating the CH-liposome with GUA smoothed the shape and made the structure more regular and homogeneous. In addition to all this, the DLS technique used in the size measurement mentioned above uses the hydrodynamic diameter measurement and aqueous medium to affect the size measurement. Although this is the reason for the difference between the size determined by FE-SEM and the size determined by DLS, the size determined by FE-SEM provides more accurate results. Liposome formulations were lyophilized before their morphology was assessed. However, it is also seen that lyophilization of liposomal formulations causes distortions in their shape.

In vitro drug release study

The drug release profile of the liposome formulations is shown in Fig. 4. The AO extract, which was used as a control in the drug release study, reached 100% GA release at 240 min. In the same period, the O-liposome reached 43.15% drug release, the CH-liposome 30.25%, and the GUA-CH-liposome 22.47%. At the end of 300 min, the drug release of O-liposome is 48.12%, CH-liposome is 32.36%, and GUA-CH-liposome is 23.84%. Encapsulation of GA in the liposome reduced the release of GA by more than 50%. The coating process of the O-liposome with CH and then GUA reduced the GA release by more than 60% and 70%, respectively. Similarly, Jeon et al. [50] reported in the in vitro release study of hyaluronate-chitosan coated liposomes that the uncoated liposome released the drug much more rapidly than the CH-coated liposome, and the first polymeric coating

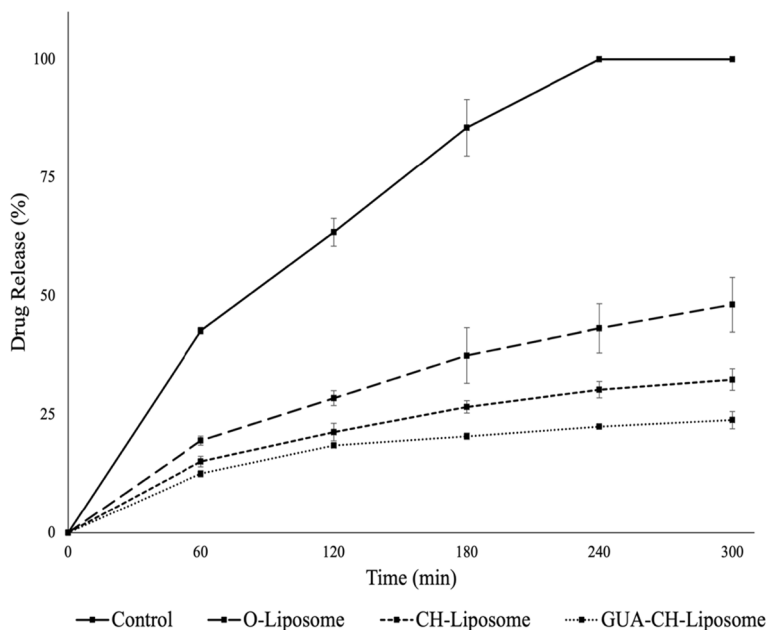


Fig. 4 In vitro drug release (%) of control, O-liposome, CH-liposome, and GUA-CH-liposome

on the liposome surface was an important factor in preventing the rapid release of the drug in the liposome. The drug release rate of liposomes varies depending on the fluidity of the lipid bilayer, hence the membrane permeability [51]. The coating of the liposome surface with polyelectrolyte biopolymer formed a more dense and thick layer on the surface, reducing the fluidity of the liposome and thus the permeability of the lipid membrane, thereby slowing down the drug release rate. These results indicate that encapsulation and LbL coating of GA reduces and controls its release in a simulated physiological environment. Improving the release profile of bioactive components such as GA is an important factor in increasing their bioavailability.

Stability study

The results of the stability study of the liposome formulations are shown in Fig. 5. The initial (Day 0) drug loading capacity of the liposome formulations was $93.77 \pm 0.05\%$ for all three conditions. The drug loading capacity for the O-liposome was $67.01 \pm 0.03\%$ at $+4\text{ }^{\circ}\text{C}$, $67.03 \pm 0.44\%$ at room temperature and $87.32 \pm 0.94\%$ at $-24\text{ }^{\circ}\text{C}$ (Day 28); for CH-liposome was $79.99 \pm 1.13\%$ at $+4\text{ }^{\circ}\text{C}$, $81.12 \pm 0.53\%$ at room temperature and $90.43 \pm 3.26\%$ at $-24\text{ }^{\circ}\text{C}$ (Day 28); for GUA-CH-liposome was $92.72 \pm 0.51\%$ at $+4\text{ }^{\circ}\text{C}$, $93.09 \pm 0.01\%$ at room temperature and $93.15 \pm 0.01\%$ at $-24\text{ }^{\circ}\text{C}$ (Day 28). Conventional liposomes generally have low stability and

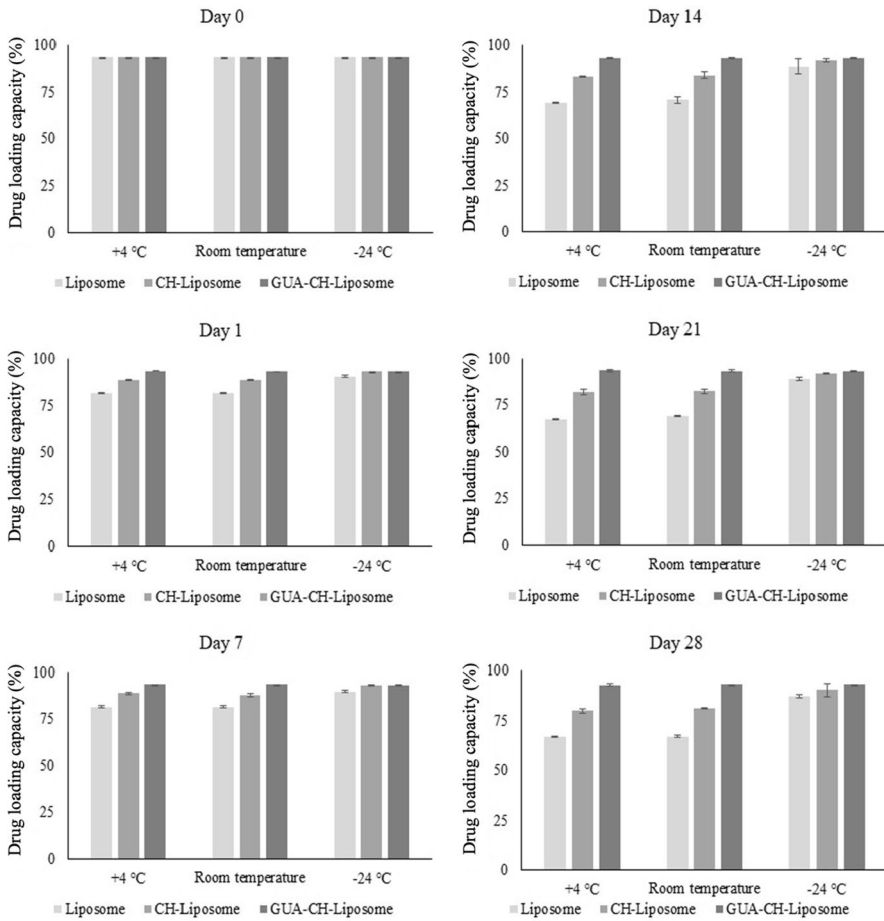


Fig. 5 Stability of O-liposome, CH-liposome, and GUA-CH-liposome at day 28

strength. Modifying the liposome surface with polyelectrolytes can be a solution to deal with these negative properties of liposomes [52]. According to the results of the stability study, coating the O-liposome with one layer generated approx. 13% difference in drug loading capacity between O-liposome and CH-liposome, and coating with two layers approx. 26% difference between O-liposome and GUA-CH-liposome at +4 °C, and the coating of liposomes significantly changed and improved their stability. The stability of all liposomes, regardless of their modification, is higher at lower temperature – 24 °C than high temperature + 4 °C.

Conclusion

In this study, nano-sized galangin-loaded polyelectrolyte liposomes were developed with a combination of thin-film hydration and LbL deposition techniques. The optimum liposome formulation was determined by optimizing various factors for liposome formation with RSM-CCD and produced with an encapsulation efficiency of $93.77 \pm 0.05\%$. The O-liposome was coated with the polyelectrolyte biopolymer chitosan and gum arabic. The GUA-CH-liposome obtained as a result of coating the O-liposome with a polyelectrolyte was 266.60 ± 8.49 nm in size, 567 ± 113 nm in hydrodynamic size, and neutral liposome with -6 mV zeta potential. According to the *in vitro* release and stability studies, the polyelectrolyte improved the release profile and stability of the O-liposome with each layer added. The final product, nano-sized galangin-loaded polyelectrolyte liposome, is an alternative carrier system suitable for use in many different targets and conditions due to its characteristic features, e.g., small size, spherical shape, neutral surface charge, improved release profile, and superior stability. The ease of generation and high encapsulation efficiency of the polyelectrolyte-coated liposomal system that has been developed, combined with the ability of liposomes to encapsulate both hydrophobic and hydrophilic compounds, show that this system can be applied to many phenolic compounds, not only galangin.

Funding The authors did not receive support from any organization for the submitted work.

Declarations

Conflict of interest The authors have no competing interests to declare that are relevant to the content of this article.

References

1. Liang X, Wang P, Yang C et al (2021) Galangin inhibits gastric cancer growth through enhancing STAT3 mediated ROS production. *Front Pharmacol* 12:646628. <https://doi.org/10.3389/fphar.2021.646628>
2. Fang D, Xiong Z, Xu J et al (2019) Chemopreventive mechanisms of galangin against hepatocellular carcinoma: a review. *Biomed Pharmacother* 109:2054–2206. <https://doi.org/10.1016/j.biopha.2018.09.154>
3. Abubakar IB, Malami I, Yahaya Y, Sule SM (2018) A review on the ethnomedicinal uses, phytochemistry and pharmacology of *Alpinia officinarum* Hance. *J Ethnopharmacol* 224:45–62. <https://doi.org/10.1016/j.jep.2018.05.027>
4. Jeong D, Kim HK, Jeong JP et al (2016) Cyclophorase/cellulose hydrogels as an efficient delivery system for galangin, a hydrophobic antibacterial drug. *Cellulose* 23:2609–2625. <https://doi.org/10.1007/s10570-016-0975-1>
5. Subramani T, Ganapathyswamy H (2020) An overview of liposomal nano-encapsulation techniques and its applications in food and nutraceutical. *J Food Sci Technol* 57:3545–3555. <https://doi.org/10.1007/s13197-020-04360-2>
6. Witika BA, Makoni PA, Matafwali SK et al (2021) Enhancement of biological and pharmacological properties of an encapsulated polyphenol: curcumin. *Molecules* 26:4244. <https://doi.org/10.3390/molecules26144244>

7. Saifullah M, Shishir MRI, Ferdowsi R et al (2019) Micro and nano encapsulation, retention and controlled release of flavor and aroma compounds: a critical review. *Trends Food Sci Technol* 86:230–251. <https://doi.org/10.1016/j.tifs.2019.02.030>
8. Shishir MRI, Xie L, Sun C et al (2018) Advances in micro and nano-encapsulation of bioactive compounds using biopolymer and lipid-based transporters. *Trends Food Sci Technol* 78:34–60. <https://doi.org/10.1016/j.tifs.2018.05.018>
9. Witika BA, Makoni PA, Matafwali SK et al (2020) Biocompatibility of biomaterials for nanoencapsulation: current approaches. *Nanomaterials* 10:1–40. <https://doi.org/10.3390/nano10091649>
10. Liu G, Hou S, Tong P, Li J (2022) Liposomes: preparation, characteristics, and application strategies in analytical chemistry. *Crit Rev Anal Chem* 52:392–412. <https://doi.org/10.1080/10408347.2020.1805293>
11. Nguyen TA, Tang QD, Doan DCT, Dang MC (2016) Micro and nano liposome vesicles containing curcumin for a drug delivery system. *Adv Nat Sci Nanosci and Nanotechnol* 7:035003. <https://doi.org/10.1088/2043-6262/7/3/035003>
12. Balakrishnan KRRP, Gopi S (2022) Systematic review on activity of liposomal encapsulated antioxidant, antibiotics, and antiviral agents. *J Liposome Res* 8:1–14. <https://doi.org/10.1080/08982104.2021.2024568>
13. Akhavan S, Assadpour E, Katouzian I, Jafari SM (2018) Lipid nano scale cargos for the protection and delivery of food bioactive ingredients and nutraceuticals. *Trends Food Sci Technol* 74:132–146. <https://doi.org/10.1016/j.tifs.2018.02.001>
14. Su C, Liu Y, He Y, Gu J (2018) Analytical methods for investigating in vivo fate of nanoliposomes: a review. *J Pharm Anal* 8:219–225. <https://doi.org/10.1016/j.jpha.2018.07.002>
15. Apolinário AC, Hauschke L, Nunes JR, Lopes LB (2021) Lipid nanovesicles for biomedical applications: ‘what is in a name’? *Prog Lipid Res* 82:101096. <https://doi.org/10.1016/j.plipres.2021.101096>
16. Aguilar-Pérez KM, Avilés-Castrillo JI, Medina DI et al (2020) Insight into nanoliposomes as smart nanocarriers for greening the twenty-first century biomedical settings. *Front Bioeng Biotechnol* 8:579536. <https://doi.org/10.3389/fbioe.2020.579536>
17. Trucillo P, Campardelli R, Reverchon E (2020) Liposomes: From bangham to supercritical fluids. *Processes* 8:1022. <https://doi.org/10.3390/pr8091022>
18. Enaru B, Socaci S, Farcas A et al (2021) Novel delivery systems of polyphenols and their potential health benefits. *Pharmaceuticals* 14:946. <https://doi.org/10.3390/ph14100946>
19. Tan C, Wang J, Sun B (2021) Biopolymer-liposome hybrid systems for controlled delivery of bioactive compounds: Recent advances. *Biotechnol Adv* 48:107727. <https://doi.org/10.1016/j.biotechadv.2021.107727>
20. Li J, Zhai J, Dyett B et al (2021) Effect of gum arabic or sodium alginate incorporation on the physicochemical and curcumin retention properties of liposomes. *LWT* 139:110571. <https://doi.org/10.1016/j.lwt.2020.110571>
21. Ahmed KS, Hussein SA, Ali AH et al (2019) Liposome: composition, characterisation, preparation, and recent innovation in clinical applications. *J Drug Target* 27:742–761. <https://doi.org/10.1080/1061186x.2018.1527337>
22. Kumar S, Dutta J, Dutta PK, Koh J (2020) A systematic study on chitosan-liposome based systems for biomedical applications. *Int J Biol Macromol* 160:470–481. <https://doi.org/10.1016/j.jbiomac.2020.05.192>
23. Sabry S, El Hakim Ramadan A, Abd elghany M et al (2021) Formulation, characterization, and evaluation of the anti-tumor activity of nanosized galangin loaded niosomes on chemically induced hepatocellular carcinoma in rats. *J Drug Deliv Sci Technol* 61:102163. <https://doi.org/10.1016/j.jddst.2020.102163>
24. Patil S, Ujalambkar V, Rathore A et al (2019) Galangin loaded galactosylated pluronic F68 polymeric micelles for liver targeting. *Biomed Pharmacother* 112:108691. <https://doi.org/10.1016/j.biopha.2019.108691>
25. Hajipour H, Nouri M, Ghorbani M et al (2021) Targeted nanostructured lipid carrier containing galangin as a promising adjuvant for improving anticancer effects of chemotherapeutic agents. *Naunyn-Schmiedeberg's Arch Pharmacol* 394:2353–2362. <https://doi.org/10.21203/rs.3.rs-600166/v1>
26. Zhu J, Wang Q, Li H et al (2018) Galangin-loaded, liver targeting liposomes: Optimization and hepatoprotective efficacy. *J Drug Deliv Sci Technol* 46:339–347. <https://doi.org/10.1016/j.jddst.2018.05.034>

27. Li Y, Guo M, Lin Z et al (2018) Multifunctional selenium nanoparticles with Galangin-induced HepG2 cell apoptosis through p38 and AKT signalling pathway. *R Soc Open Sci* 5:180509. <https://doi.org/10.1098/rsos.180509>
28. Yao H, Lu H, Zhang J et al (2019) Preparation of prolonged-circulating galangin-loaded liposomes and evaluation of antitumor efficacy in vitro and pharmacokinetics in vivo. *J Nanomater*. <https://doi.org/10.1155/2019/7236895>
29. Li CY, Cheng SE, Wang SH et al (2021) The anti-inflammatory effects of the bioactive compounds isolated from *Alpinia officinarum* Hance mediated by the suppression of NF-kappaB and MAPK signaling. *Chin J Physiol* 64:32–42. https://doi.org/10.4103/CJP.CJP_81_20
30. Karkar B, Şahin S (2022) Determination of phenolic compounds profiles and antioxidant properties of oleaster (*Elaeagnus angustifolia* L.) grown in Turkey. *Eur Food Res Technol* 248:219–241. <https://doi.org/10.1007/s00217-021-03875-y>
31. Şahin S, Nasir NTBM, Erken I et al (2019) Antioxidant composite films with chitosan and carotenoid extract from *Chlorella vulgaris*: Optimization of ultrasonic-assisted extraction of carotenoids and surface characterization of chitosan films. *Mater Res Express* 6:095404. <https://doi.org/10.1088/2053-1591/ab2def>
32. Cui T, Jia A, Yao M et al (2021) Characterization and caco-2 cell transport assay of chito-oligosaccharides nano-liposomes based on layer-by-layer coated. *Molecules* 26:4144. <https://doi.org/10.3390/molecules26144144>
33. Men W, Zhu P, Dong S et al (2020) Layer-by-layer pH-sensitive nanoparticles for drug delivery and controlled release with improved therapeutic efficacy in vivo. *Drug Deliv* 27:180–190. <https://doi.org/10.1080/10717544.2019.1709922>
34. Xiong Y, Guo D, Wang L et al (2009) Development of nobilside A loaded liposomal formulation using response surface methodology. *Int J Pharm* 371:197–203. <https://doi.org/10.1016/j.ijpharm.2008.12.031>
35. Hashemi SH, Montazer M, Naghdi N, Toliyat T (2018) Formulation and characterization of alprazolam-loaded nanoliposomes: screening of process variables and optimizing characteristics using RSM. *Drug Dev Ind Pharm* 44:296–305. <https://doi.org/10.1080/03639045.2017.1391834>
36. Refaat H, Mady FM, Sarhan HA et al (2021) Optimization and evaluation of propolis liposomes as a promising therapeutic approach for COVID-19. *Int J Pharm* 592:120028. <https://doi.org/10.1016/j.ijpharm.2020.120028>
37. Deniz A, Sade A, Severcan F et al (2010) Celecoxib-loaded liposomes: Effect of cholesterol on encapsulation and in vitro release characteristics. *Biosci Rep* 30:365–373. <https://doi.org/10.1042/BSR20090104>
38. Maja L, Željko K, Mateja P (2020) Sustainable technologies for liposome preparation. *J Supercrit Fluids* 165:104984. <https://doi.org/10.1016/j.supflu.2020.104984>
39. Rasmussen MK, Pedersen JN, Marie R (2020) Size and surface charge characterization of nanoparticles with a salt gradient. *Nat Commun* 11:2337. <https://doi.org/10.1038/s41467-020-15889-3>
40. Wang DY, van der Mei HC, Ren Y et al (2020) Lipid-based antimicrobial delivery-systems for the treatment of bacterial infections. *Front Chem* 7:872. <https://doi.org/10.3389/fchem.2019.00872>
41. Barbosa JAC, Abdelsadig MSE, Conway BR, Merchant HA (2019) Using zeta potential to study the ionisation behaviour of polymers employed in modified-release dosage forms and estimating their pKa. *Int J Pharm X* 1:100024. <https://doi.org/10.1016/j.ijpx.2019.100024>
42. Wang Y (2021) Liposome as a delivery system for the treatment of biofilm-mediated infections. *J Appl Microbiol* 131:2626–2639. <https://doi.org/10.1111/jam.15053>
43. Danaei M, Dehghankhold M, Ataei S et al (2018) Impact of particle size and polydispersity index on the clinical applications of lipidic nanocarrier systems. *Pharmaceutics* 10:57. <https://doi.org/10.3390/pharmaceutics10020057>
44. Wen MM, Farid RM, Kassem AA (2014) Nano-proniosomes enhancing the transdermal delivery of mefenamic acid. *J Liposome Res* 24:280–289. <https://doi.org/10.3109/08982104.2014.911313>
45. Perez-Ruiz AG, Ganem A, Olivares-Corichi IM, García-Sánchez JR (2018) Lecithin-chitosan-TPGS nanoparticles as nanocarriers of (-)-epicatechin enhanced its anticancer activity in breast cancer cells. *RSC Adv* 8:34773–34782. <https://doi.org/10.1039/c8ra06327c>
46. Tavares L, Noreña CPZ (2020) Encapsulation of ginger essential oil using complex coacervation method: coacervate formation, rheological property, and physicochemical characterization. *Food Bioproc Tech* 13:1405–1420. <https://doi.org/10.1007/s11947-020-02480-3>

47. Hernández-Fernández MÁ, García-Pinilla S, Ocampo-Salinas OI et al (2020) Microencapsulation of vanilla oleoresin (*V. Planifolia andrews*) by complex coacervation and spray drying: Physicochemical and microstructural characterization. *Foods* 9:1375. <https://doi.org/10.3390/foods9101375>
48. Rajabi H, Jafari SM, Rajabzadeh G et al (2019) Chitosan-gum Arabic complex nanocarriers for encapsulation of saffron bioactive components. *Colloids Surf A Physicochem Eng Asp* 578:123644. <https://doi.org/10.1016/j.colsurfa.2019.123644>
49. Zhang T, Su M, Jiang X et al (2019) Transepithelial transport route and liposome encapsulation of milk-derived ACE-inhibitory peptide Arg-Leu-Ser-Phe-Asn-Pro. *J Agric Food Chem* 67:5544–5551. <https://doi.org/10.1021/acs.jafc.9b00397>
50. Jeon S, Yoo CY, Park SN (2015) Improved stability and skin permeability of sodium hyaluronate-chitosan multilayered liposomes by Layer-by-Layer electrostatic deposition for quercetin delivery. *Colloids Surf B Biointerfaces* 129:7–14. <https://doi.org/10.1016/j.colsurfb.2015.03.018>
51. Li N, Zhuang C, Wang M et al (2009) Liposome coated with low molecular weight chitosan and its potential use in ocular drug delivery. *Int J Pharm* 379:131–138. <https://doi.org/10.1016/j.ijpharm.2009.06.020>
52. Hermal F, Frisch B, Specht A et al (2020) Development and characterization of layer-by-layer coated liposomes to increase their resistance in biological media. *Int J Pharm* 586:119568. <https://doi.org/10.1016/j.ijpharm.2020.119568>

Publisher's Note Springer Nature remains neutral with regard to jurisdictional claims in published maps and institutional affiliations.

Springer Nature or its licensor (e.g. a society or other partner) holds exclusive rights to this article under a publishing agreement with the author(s) or other rightsholder(s); author self-archiving of the accepted manuscript version of this article is solely governed by the terms of such publishing agreement and applicable law.

Authors and Affiliations

Büşra Karkar¹  · İlkyaz Patr¹  · Saliha Şahin¹ 

✉ Saliha Şahin
salihabilgi@uludag.edu.tr

Büşra Karkar
busraakarkar@gmail.com

İlkyaz Patr
ilkyazpatir@gmail.com

¹ Department of Chemistry, Faculty of Science and Arts, Bursa Uludag University, Bursa, Türkiye